



HAL
open science

Alkaline Pretreatments for Sorghum and Miscanthus Anaerobic Digestion: Impacts at Cell Wall and Tissue Scales

Hélène Laurence Thomas, Helga Felix P. Nolasco, Hélène Carrère, Marc Lartaud, Tuong-Vi Cao, Christelle Baptiste, Jean-Luc Verdeil

► **To cite this version:**

Hélène Laurence Thomas, Helga Felix P. Nolasco, Hélène Carrère, Marc Lartaud, Tuong-Vi Cao, et al.. Alkaline Pretreatments for Sorghum and Miscanthus Anaerobic Digestion: Impacts at Cell Wall and Tissue Scales. *BioEnergy Research*, 2022, 15, 10.1007/s12155-021-10342-9 . hal-03539190

HAL Id: hal-03539190

<https://hal.inrae.fr/hal-03539190>

Submitted on 4 Sep 2023

HAL is a multi-disciplinary open access archive for the deposit and dissemination of scientific research documents, whether they are published or not. The documents may come from teaching and research institutions in France or abroad, or from public or private research centers.

L'archive ouverte pluridisciplinaire **HAL**, est destinée au dépôt et à la diffusion de documents scientifiques de niveau recherche, publiés ou non, émanant des établissements d'enseignement et de recherche français ou étrangers, des laboratoires publics ou privés.

Alkaline pretreatments for sorghum and miscanthus anaerobic digestion: impacts at cell wall and tissue scales

Hélène Laurence Thomas¹, Helga Felix P. Nolasco¹, Hélène Carrère^{1,*}, Marc Lartaud^{2,3}, Tuong-Vi Cao^{2,3}, Christelle Baptiste^{2,3}, Jean-Luc Verdeil^{2,3}

¹ INRAE, Univ Montpellier, LBE, 102 avenue des Etangs, 11100 Narbonne, France

² PHIV, CIRAD, UMR AGAP Institut, F-34398 Montpellier, France

³UMR AGAP Institut, Univ Montpellier, CIRAD, INRAE, Institut Agro, F-34398 Montpellier, France

*corresponding author: helene.carrere@inrae.fr

Abstract

Lignocellulosic biomass is hardly degraded during anaerobic digestion. Amongst a large panel of pretreatments used to improve the biodegradability of this substrate, alkaline pretreatments are recognized as the most efficient to remove lignin and therefore improve the methane production of these substrates. This article uses different histological stains (FASGA, phloroglucinol, Mäule reagent, Congo red), immunolocalization and histological quantification on pretreated internode stem tissues section in order to decipher the mechanism of alkaline pretreatment action (CaO and NaOH) in the anatomical and lignocellulosic matrix scale of Sorghum Biomass 140 hybrid and of *Miscanthus x giganteus* Floridulus. A significant delignification of all tissues was observed (sclerenchyma, parenchyma and xylem) except in the epidermis and in the internal part of the perivascular sclerenchyma. The degradation of lignin under the effect of alkaline pretreatment is accompanied by a massive unmasking of cellulose and a reduction of crystalline cellulose. This induced an increase of anaerobic digestion kinetics for both biomass and of methane yield for miscanthus. Miscanthus is rich in G-type lignins located mainly at the level of the perivascular sclerenchyma of the external

internode zone which was more degraded by alkalies than the S-type lignin, this may explain the improvement of miscanthus methane potential.

Keywords: alkaline pretreatments; lignocellulosic biomass; biogas; histochemistry; tissue structure; cell wall macromolecules mapping.

Introduction

Because of greenhouse gas emissions linked to the exploitation of fossil resources, it is necessary to find sustainable alternatives to meet the energy and product needs of industries and populations. The lignocellulosic biomass is being further explored as a main substrate in biorefinery domain [1]. Amongst the lignocellulosic substrates, miscanthus and sorghum (two C4 fast growing monocots) are interesting options as *M. x giganteus* can produce high level of aboveground biomass with a low environmental impact [2]. As for sorghum which has a high biomass yield potential (even under limited water supplies), is easy of cultivation and widely adapted to high temperatures, low water supplies and poor soils [3].

These two biomass samples are mainly composed of cellulose, hemicelluloses and lignin [4]. The two first components can be grouped under the term holocelluloses. The cellulose is a paracrystalline structure formed of β -(1 \rightarrow 4)-D-glucan chains, which are synthesized individually and can crystallize into cellulose microfibrils through inter- and intramolecular hydrogen bonds and Van der Waals bonds. Because cellulose is the main load-bearing polymer of the cell wall, the length, angle, and crystallinity of cellulose microfibrils are important determinants of the physical characteristics of the cell wall [5]. The hemicellulose is a polysaccharide composed of heteromannans, xyloglucan, heteroxylans, and mixed-linkage glucans [6]. Unlike cellulose, hemicellulose frequently has side chain groups and are essentially amorphous [7]. The amorphous and branched properties make hemicelluloses more susceptible to biological, thermal, and chemical hydrolysis into their monomer compounds. During hydrolysis, the moisture content, pH, and temperature are the most critical parameters to be observed when taking into account only hemicelluloses [8]. Lignin is an aromatic polymer. The main building blocks of lignin are the hydroxycinnamyl alcohols (or monolignols), coniferyl alcohol and sinapyl alcohol, with typically minor amounts of p-coumaryl alcohol. The units resulting from the monolignols, when incorporated into the lignin polymer, are called guaiacyl

(G), syringyl (S), and p-hydroxyphenyl (H) units [9]. Baucher et al. (1998) mentioned that in monocots, the H, G and S units proportions in lignins are 2-15%, 35-80% and 20-61%, respectively. In the case of mature maize, the proportions of G, S and H units are 35, 61 and 4% [10]. Lignin is deposited secondarily in the cell wall and provides the wall with rigidity, water impermeability and high resistance to decomposition [11]. In addition, lignin is not homogeneously distributed within the biomass and its distribution depends closely on the cellular and tissue structure of the biomass.

The lignocellulosic biomass are good candidates for anaerobic digestion. In fact, the sugars contained in cellulose and hemicellulose have been shown to be anaerobically biodegradable [12]. Because it is cross-linked with the other cell wall components, lignin minimizes the accessibility of cellulose and hemicellulose to microbial enzymes, leading to a reduced digestibility of biomass [13]. These bonds, called lignin-carbohydrate complex (LCC), form a complex and compact structure [14]. However, this structure makes the lignocellulosic biomass recalcitrant to bioconversion [15]. The aim of pretreatments is to break down lignin and LCC, disarrange the crystalline structure of cellulose and expose holocellulose, meanwhile made easier the hydrolysis of polysaccharides [16]. Indeed, to increase the accessibility of lignocellulosic biomass for further enzymatic hydrolysis, Rollin et al. (2011) proved that lignin removal is not sufficient [17]. The crystallinity of the cellulose has to decrease as well. In the same way, Monlau et al. (2012) reported that, after lignin content, crystalline cellulose content was the second parameter impacting negatively the methane yield during anaerobic digestion (AD) [18].

Lignocellulosic pretreatments (chemical, physical, biological and physicochemical) are widely applied in literature [19]. Amongst them, alkaline pretreatments are recognized as the most efficient to remove the lignin [20]. They are also known to decrease the crystallinity structure of cellulose [21]. Various reagents were used (NaOH, Na₂CO₃, Ca(OH)₂, NH₄OH) in

literature [22]. In a previous study on *Miscanthus x giganteus*, at identical pretreatment conditions, NaOH was more efficient than CaO [23]. Consequently, the performance of alkaline pretreatment was different according to the alkali used. However, taking into account the valorization of the digestate after AD in agricultural soil and considering the issue of soil salinity, CaO is the preferred reagent. Their impacts are mainly studied on the methane production yield, the first order kinetics (e.g. sunflower stalks [20]), the biochemical composition (e.g. miscanthus [24]) and the crystallinity index. Positive impacts of alkali pretreatments on anaerobic digestion of various lignocellulosic substrates have been reported. Monlau et al. (2012) applied alkali at 4 g.100 g_{TS}⁻¹ dose for 24 h at 55°C to sunflower stalks; the methane potential increased by 26 and 35% with Ca(OH)₂ and NaOH, respectively [20]. Sambusti et al. (2013) applied NaOH pretreatment at 10 g.100 g_{TS}⁻¹ on five sorghum genotypes; the impact on the methane yields ranged from 0 to 7% of increase [25]. Nkemka et al. (2016) studied the effect of CaO or NaOH at 6 g.100 g_{VSadded}⁻¹ for 24 h at 70°C on *Miscanthus × giganteus*; the methane yield increased by 39% and 60% respectively [26].

The recalcitrance of the plant cell wall to anaerobic digestion is a multi-scale phenomenon covering several orders of magnitude encompassing both the macromolecular barriers of the cell wall (i.e. crystalline cellulose or lignin carbohydrate complex) and also cellular factors. Indeed, the distribution of lignin, cellulose and hemicellulose is not uniform in the tissues cells. For example, a lignified cell of sclerenchyma fiber has a thick lignified wall with a small diameter lumen in the center, whereas lignified parenchyma cells or xylem vessels that conduct the raw sap have thinner lignified cell walls and a larger diameter center lumen providing more surface area for contact with anaerobic micro-organisms and to alkaline pretreatment solution.

It has been suggested that microscopic analysis of the lignocellulosic biomass and comparisons in between pretreated and untreated samples can be used to qualitatively predict

and understand the susceptibility of the lignocellulosic materials to subsequent degradation [27].

Since the properties of the biomass also depend not only on its biochemical composition but also on its cell architecture, its anatomical and tissue composition must be taken into account. Despite the importance of visualizing cellular scale to fully understand the effect of biomass pretreatments, no histochemical studies have been conducted for this purpose. FASGA staining combined with image processing has been demonstrated to be a powerful tool to analyze lignocellulosic biomass cellular structures and tissues as it was recently applied to study stems of maize [25] and miscanthus [26]. This method of evaluation could bring highly valuable information about the mechanisms of the alkaline pretreatments.

The present work aims to understand the effect of two alkaline reagents on the anatomical structure of sorghum and miscanthus stem internodes. For the first time, the use of FASGA staining provided a histological quantification of the effects of alkaline pretreatments and successfully linked them to the improvement of the performance of anaerobic digestion. To complete this work, a comparative study of the mapping of the main components of the cell wall (cellulose, crystalline cellulose, lignin, G and S lignin) was carried out through histochemical methods before and after pretreating the internodes.

These histochemical observations are consistent with biochemical data and provide new insight about the effects of alkaline pretreatments on the cellular component of biomass and methane production from sorghum and miscanthus.

Material and Methods

1. Plant material

Miscanthus x giganteus Floridulus was grown in the INRA experimental unit located in Estrées-Mons in the North of France (49°53 N, 3°00 E) and harvested in the winter of 2018 in its 12th year at the end of winter at over-maturity [2]. *Sorghum bicolor* L. Moench Biomass 140 hybrid was grown in CIRAD of Montpellier (43°39 N, 3°52 E) located in South of France and harvested in the summer of 2015 at the dough grain stage [28]. The stems were dried in the field and stored at room temperature. The TS and volatile solids (VS) content of sorghum stalk were 91% and 94%_{TS}, respectively. Those of miscanthus were 94% and 98%_{TS}, respectively.

2. Substrate preparation

The internodes of sorghum and miscanthus were first transversally cut into cylinders (1 cm in length) using a scroll saw (65 W, 1440 round-trip /Min, Castorama-France). They were then transversally cut to 115 µm and 110 µm sections respectively, using a Vibratome (Microm HM650V Germany). The cylindrical sections were collected and stored at 4°C in ethanol 70% solution before alkali pretreatment or histological analysis. For biochemical analysis and BMP (Biochemical Methane Potential) measurements, the dried internodes were cut into 2 mm sections using a scroll saw (65W, 1440 round-trip /Min, Castorama-France).

3. Alkaline pretreatments

Soda (NaOH, Sigma) and lime (CaO, Akdolit[®] Q90; purity ≥ 92%) pretreatments were carried out in 40 mL flasks containing 3-4 sections of each biomass internodes. The alkali dose was 10g.100g_{TS}⁻¹. Flasks were put on a thermostated mixing table, the mixing speed was 90 RPM and the total length of pretreatment was 24 hours. The pretreatment's temperature was 26 or 55 °C. Temperature of 26°C was selected because it is close to ambient temperature, it can thus represent a pretreatment with no heat requirements as used in Thomas et al. (2019)[23]. However, we preferred to control temperature at 26°C in order to avoid small impacts of room temperature variations. 55°C is the common temperature used in thermophilic anaerobic

digestion process. Pretreatments at this temperature showed higher efficiency than 30°C pretreatments in the case of sunflower stalks [20] or than 40°C pretreatments of ensiled sorghum [29]. Moreover, in an energy saving and agricultural AD context, higher temperatures were not studied. After sampling, the sections were rinsed three times with distilled water, once with a phosphate buffer solution (pH 7.2, 0.2 M) and once with distilled water. The phosphate solution neutralizes the pH to ensure that the following staining procedure will not compromise the alkaline pretreatment.

In order to study the kinetics of the pretreatment on the tissues, miscanthus and sorghum pretreated samples were collected at different pretreatment lengths (every 30 minutes or every few hours until 24h and then at 48h, 96h and 144h). Sorghum was tested initially in order to better understand the pretreatment impacts, as these were more abundant for testing than miscanthus. After initial observations, pretreatment lengths were decided and it was no longer necessary to sample as frequently.

4. Internode Histochemical Analyses

4.1 Staining and immunolocation of transverse histological sections of internodes

For FASGA staining, the internode cuts were stained overnight using a FASGA solution diluted in distilled water (1:7, v/v). The FASGA mother solution is composed of 3% of safranin solution, 21% of Alcian blue solution, 1.5% of acetic acid, 45.2% of glycerin and 29.3% distilled water prepared according to [26]. The safranin (a red, basic, cationic dye) stains the lignified cell walls in red, and Alcian blue (an acidic anionic dye) stains the pectocellulosic cell walls in blue. The main advantage of FASGA staining is that lignin and cellulose can be visualized in a single slide. However, because FASGA is not highly specific to lignin or cellulose, other complementary staining methods were employed.

The Phloroglucinol-HCl (Wiesner) staining is specific to lignin and stains only them [30]. Histological internode cuts were immersed in a solution of ethanol saturated with phloroglucinol (Sigma, P3502-25G) at 2% for 5 minutes. Later, they are placed on a glass slide and a few drops of a solution of a hydrochloric acid solution (HCl) (Sigma, 07102_1L_D) at 18% are poured on to it, in order to immerse the entire section. A red color appears immediately in the presence of lignin.

For Mäule staining, the cuts were placed into a 1% potassium permanganate solution for 5 minutes at room temperature. After rinsing twice with distilled water, sections are transferred into 18% of HCl solution until the strong brown color is reduced. The lignin staining is revealed after an immersion of the slices in a 20% ammoniac aqueous solution. The Mäule staining is specific towards Syringyle (S) lignin units and can be used to differentiate lignin enrichments in S or Guaiacyl (G) units (stained in red and brown/yellow, respectively) [31]. Observations with the microscope must be undertaken immediately as the staining is only visible for a short period of time.

For Congo red staining, the sections were submerged in 0.1% Congo red solution for 5 minutes and then rinsed in distilled water.

Crystalline cellulose was visualized using a cellulose-directed carbohydrates-binding module (CBM) (ref CBM3a from Plant Probes). The experimental procedure was done according to literature [32, 33]. Cuts were saturated with BSA (Bovine Serum Albumine) solution (5% in phosphate-buffered saline) (PBS) overnight to prevent non-specific binding, rinsed with PBS and then left for incubation for 1.5 hours at room temperature in a CBM solution (1:50 dilution in PBS solution). After four rinses with PBS (10 minutes each), the sections were incubated with an anti CBM mouse antibody (Molecular Probes) used at 1:100 dilution in PBS and BSA 3% solution for 3 h at room temperature. A four-step rinse with PBS

was repeated. Anti-his mouse Alexa Fluor 546 (Molecular Probes) in a 1:1000 dilution in PBS for 1.5h was used as a secondary antibody.

For all staining methods applied, histological cuts were assembled between glass slide and cover-slip in an aqueous glycerol solution (50/50, V/V).

4.2 Image acquisition

Histological sections stained with FASGA solution were scanned and digitalized at 20X magnification using a Nanozoomer XR (Hamamatsu, Photonics Ltd., Hertfordshire, UK). Images can be viewed using a NDPI viewer from Hamamatsu (Hamamatsu, Photonics Ltd., Hertfordshire, UK at <https://www.hamamatsu.com/eu/en/product/type/U12388-01/index.html>).

The phloroglucinol, Maïle and Congo Red stained sections were digitized using an upright Nikon Ni-E microscope (Objective 20) equipped with a color camera DS-Ri2.

Immunofluorescence imaging of crystalline cellulose epitopes was performed using an up-right LSM 800 confocal microscope (Zeiss) with a 40X objective (LD C-Apo 1.1NA W), excitation wavelength: 561 nm.

4.3 Image processing of FASGA stained sections

A specific macro toolset (PHIVSorghum Biotool set) described by Perrier et al. (2017) was developed [34], running on the 1.48 (or higher) version of ImageJ (<http://imagej.nih.gov/ij/download.html>). The macro works by segmenting areas on the internode sections, divided in two zones (external zone Z1 and internal zone Z2, Figure 1). As shown in Figure 1, %Z1 and %Z2 indicate the percentage of Z1 and Z2 areas respectively, PercSclZ1 represents the percentage of red Sclerenchyma area in Zone 1; densVBZ2 represents the density of vascular bundles and finally PercbluZ2 shows the amount of blue areas in Z2.

The focus of this study was on the percentage of the area that remains in red after pretreatment in Z1 (representing mainly the lignified sclerenchyma area), and the percentage of parenchyma cell wall areas that turns blue in Z2 (representing the cellulosic material).

Fig. 1: Example of image processing under ImageJ of sorghum transversal internode section. Z1 stands for Zone 1, it is the outer internode zone characterized with a high density of vascular bundles. Z2 is the internal zone, PercSlcZ1: percentage of lignified sclerenchyma area in Z1, PercBluZ2: percentage of cellulosic area available in Z2, densVBZ2: represents the density of vascular bundles in Z2.

4.4 Measurement holocellulosic cell decay in Z2

The thickness of the cell walls between two adjacent parenchyma cells was measured using a NDPI viewer. This measurement was done in the middle of the junction and repeated 18 times in Z2.

5. Biochemical composition

The analysed samples were ground to 1 mm. The TS (Total Solids) and VS (Volatile Solids) contents were measured according to standard methods [35]. The lignin and carbohydrates (glucose, xylose and arabinose) in solid phases were measured in duplicates using the strong acid hydrolysis protocol adapted from NREL (National Renewable Energy Laboratory) acid hydrolysis method [36]. The removal of Klason lignin, cellulose and hemicellulose was calculated according the Equation 1

$$R = 100 \times \frac{\text{Quantity in raw biomass} - \text{Quantity in pretreated biomass}}{\text{Quantity in raw biomass}} \quad \text{Eq. (1)}$$

The crystallinity of the cellulose was estimated using the Lower Order Index (LOI), obtained with a Fourier transform medium infrared spectrometer, and defined by the ratio of 1430 and 898 cm^{-1} peak areas. The spectra were analysed with the Omnic software (Version 9.1). This index can be used to determine the amount of crystalline cellulose [18]

$$LOI = \frac{\textit{Crystalline cellulose}}{\textit{Amorphous cellulose}} \quad \text{Eq. (2)}$$

6. Measurement of methane potential from pretreated internodes

Pretreatments were carried out in 100 mL flask using 0.5 g_{TS} of dry biomass. For BMP tests, the flasks contained a sodium bicarbonate buffer (NaHCO₃, 50 g.L⁻¹), macro-elements and oligoelements solutions whose compositions are given by Monlau et al. (2012) [20] and anaerobic sludge (from UASB treating sugar industry wastewater (Marseille, France) at 5 g_{VS}.L⁻¹ and the substrate (raw or pretreated) at 5 g_{TS}.L⁻¹. Degasification with nitrogen was carried out to obtain anaerobic conditions. Duplicate bottles were incubated at 35°C for 60 days. The methane production was monitored by Automatic Methane Potential Test System or AMPTS (Bioprocess Control AB, Lund, Sweden). All volumes were expressed in normal conditions (0°C, 1.013 bar) and per gram of initial Volatile Solids (VS) thus, the eventual losses of organic matter during pretreatments were considered in the results. A blank test (inoculum without substrate) was carried out in triplicates to measure endogenous methane production from the inoculum. This endogenous production ranged 14% of total methane production.

7. Measurement of the first order kinetics constant

To quantify the impact of the pretreatments on the kinetics of methane production, first order kinetic constants were calculated by using least-squares fit of methane production data versus time (t) to the following equation:

$$V = V_{max}(1 - e^{-kt}) \quad \text{Eq. (3)}$$

where V is the volume of methane (NmL_{CH₄}.g_{VS}⁻¹), V_{max} the maximum producible methane volume (NmL_{CH₄}.g_{VS}⁻¹), k the first order kinetics constant (d⁻¹) and t the digestion time (d). V_{max} and k were determined using Microsoft Excel's Solver function.

8. Statistical analysis

The comparison of raw and pretreated holocellulosic cell wall thickness with each other was performed using the Tukey's Honest Significant Difference test [37].

The Principal Components Analysis (PCA) was used for studying the interdependence between the biochemical composition, the methane production, the first order kinetics constant and the two variables from the image analysis, using R software (version 3.3.2). In order to indicate the quality of the variable representation on the PCA, the \cos^2 was displayed. A high \cos^2 indicates a good representation of the variable on the main considered axes.

The analysis of variance (ANOVA) was performed with the software SAS (version 9.4). The model (Eq. 4) was performed for each biomass separately:

$$Y_{rt dk} = \mu + R_r + T_t + D_d + (RT)_{rt} + \varepsilon_{rt dk} \quad \text{Eq. (4)}$$

Where Y_{brthk} is the studied variable (PercSciZ1 or PercBluZ2) according to the pretreatment varying with the reagent r , the temperature t and the duration d . μ is the trial mean, R_r is the reagent effect (NaOH or CaO), T_t is the temperature effect (26 or 55°C), D_d is the duration of the pretreatment (from 0.5 to 144 h), $(RT)_{rt}$ is the interaction between the reagent and the temperature, and ε_{rthk} is the residual error. The index k corresponds to the k^{th} image which received the same combination Duration×Reagent×Temperature, with maximum k being 1, 2 or 3 depending on the combination of interest. This $\varepsilon_{rt dk}$ term was used as the error term in the hypothesis testing.

Results and discussion

1. Impact of alkaline pretreatments on biomass tissue, structure and histochemical characterisation of internodes

1.1 General anatomic organization plan of raw sorghum and miscanthus internodes

Figure 2 presents the raw and pretreated samples for 24h internodes stained with FASGA. The qualitative comparison between the two raw biomass show they have a similar organization plan composed of two main zones. Z1 (outer zone), composed of lignified epidermis and vascular bundles (VB) protected by a mature sclerenchyma with thick lignified cell walls. Z2 (inner zone) is composed of parenchyma cells and VB (Fig. 2).

Table 1 presents the results of image J processing carried out on raw FASGA stained internodes. The area of sorghum stems is two times larger than the area of the miscanthus stems. The zone definitions are alike, but the percentage of red sclerenchyma in Z1 and the quantity of vascular bundles are more abundant for sorghum. The outer zone (Z1) reveals higher density of fiber bundles compared to the inner zone (Z2). The density of VB decreases from the epidermis towards the internal part of the stem that has the highest density of parenchyma and these cells around the VB are rich in lignin and cellulose (Table 1). The VB distribution in Z2 is less homogeneous in miscanthus with none or very few vascular bundles in its center. The center of Z2 presents a gap in miscanthus. These observations are in accordance with previous miscanthus microscopic observations in literature [38, 39]

Fig. 2: Comparative effect of alkaline pretreatments on internode structure. For all the pretreatments, the duration was 24 hours. Observations were made after FASGA staining.

Table 1: Results of internode transverse section image processing for untreated samples (raw sorghum and miscanthus biomass) stained with FASGA. %Z1 and %Z2 indicating percentage of Z1 (external zone) and Z2 (internal zone) area respectively, PercSclZ1 representing the percentage of red Sclerenchyma areas in Zone 1; densVBZ2 indicating the density of vascular bundles and finally PercbluZ2 representing the amount of blue (tissues with pectocellulosic cell walls) area in Z2.

Biomass	Area (mm ²)	%Z1	%Z2	PercSclZ1	densVBZ2	PercBluZ2
Sorghum	68.2 ± 2.0	20.6 ± 2.1	79.4 ± 2.1	50.8 ± 5.1	1.8 ± 0.7	1.8 ± 0.6
Miscanthus	30.3 ± 1.9	21.4 ± 0.7	78.6 ± 0.7	39.9 ± 2.4	2.6 ± 0.1	3.3 ± 1.3

1.2 Influence of alkaline pretreatments on internodes tissues

1.2.1 Qualitative observations

Concerning the pretreated stem internodes, an important evolution of staining could be noticed for all the pretreatments compared with the controls. The percentage of blue staining increased noticeably (Fig. 2). There was a significant decrease in the red sclerenchyma area in Z1. This resulted in an evident color difference in the parenchymal area in Z2 that turned blue, showing that cellulose became more available. For sorghum, the lignified sclerenchyma around the vascular bundles appeared smaller. Comparing all pre-treatments applied on sorghum, the NaOH pretreatment at 55⁰C seems to have the most remarkable change in the reduction of the Z1 sclerenchyma lignified portion (Fig. 2). A strong color difference can be noticed in this area, which is almost entirely blue. For miscanthus, visually, pretreatments with CaO at 26⁰C and NaOH at 26⁰C seemed to retain a part of the red coloration in Z2, possibly because these treatments did not have such a strong effect in the lignified sclerenchyma area as pretreatment NaOH at 55⁰C (Fig. 2). As for sorghum, pretreatment with NaOH at 55⁰C seems to be the most effective. In all pretreated miscanthus samples, the center area of the section has a hole, a similar phenomenon is current with untreated miscanthus stem samples. Pretreatments seem to attack

the central parenchyma cells in the inner zone more intensely (Z1) which increases the size of the central lacuna.

In summary, the epidermis and the perivascular sclerenchyma were the less affected tissues by alkaline pretreatment. The parenchyma in Z2 was the most affected. Furthermore, these pretreatments did not affect only lignified structures as a thickening of cell walls and a separation of parenchyma cells in the Z2 were also noticed.

The thickness of the cell walls measured between two adjacent parenchyma cells on raw sorghum and miscanthus internodes were 1.41 ± 0.56 and 1.88 ± 0.43 μm , respectively. Those on sorghum internodes pretreated with CaO or NaOH at 55°C for 24h were 2.07 ± 0.54 and 2.31 ± 0.45 μm , respectively. In the case of miscanthus, it was 2.64 ± 0.49 and 3.13 ± 0.55 μm . Thus for the two types of biomass studied, the pretreatment had a significant impact on the width of the cell wall (p-value = $6.3 \cdot 10^{-6}$ and $9.5 \cdot 10^{-10}$, for sorghum and miscanthus, respectively). This cell wall thickening is often accompanied by a weakening of the parenchyma cells (Fig. 2). By contrast with sorghum, the impact of NaOH and CaO was significantly different for miscanthus internodes (p-value = 0.33 and $9.5 \cdot 10^{-3}$, respectively). Soda lead to a stronger parenchyma cell weakening.

1.2.2 Quantitative observations: FASGA staining evolution over time

The quantitative results of the kinetics study are reported in Fig. 3. Amongst the different parameters given by the image processing, PercSclZ1 and PercBluZ2 best describe the difference between the two biomass. The evolution of cellulosic parenchyma percentage of (blue staining: PercBluZ2) in Z2 increased exponentially until around 24 hours where at around 90% a plateau was achieved. The remaining 10% could correspond to the xylem and sclerenchyma unaffected by the pretreatment. Regarding sorghum, the evolution of this percentage for internodes pretreated with NaOH at 26°C was slower than the others. For

miscanthus, there were two different kinetic behaviors depending on the pretreatment temperature. Those at 55°C were faster than those at 26°C.

Fig. 3: Sorghum (S) and Miscanthus (M) biomass behavior during alkaline pretreatments: Influence of NaOH, CaO and temperature on the evolution of the cellulosic cells of the Z2 zone (PercBluZ2) (a) and on the lignified sclerenchyma in the outer internode zone (PercScIz1) (b) from 0 to 144 h. Alkaline pretreatments were carried out at 26°C and 55 °C.

The percentage of lignified sclerenchyma in Z1 (red color) (PercScIz1) decreased rapidly until 24h and then decreased at a slower rate. In the same way as PercBluZ2, the kinetics of PercScIz1 decrease was faster at 55°C than at 26°C and was faster with NaOH than with CaO. A large part of the sclerenchyma was degraded in the first 24 hours. The pretreatment with NaOH at 55°C seemed particularly efficient on sorghum.

The aforementioned observations were confirmed by ANOVA analysis (Table 2). ANOVA revealed that, for each biomass, the pretreatment duration had a significant impact, although after 24 h, PercBluZ2 evolved slightly. The interaction between the reagent and the temperature was significant for both miscanthus parameters and sorghum PercBluZ2. For sorghum PercScIz1, this interaction was not significant but the temperature and the reagent were significant. These differences highlight the different pretreatment impacts according to the biomass. In brief, the main effects of the pretreatment took place within the first day. The temperature was more impactful on sorghum and seemed to have a higher impact than the reagent, with a higher reaction kinetic at higher temperature (Table 2).

Table 2: Sources of variation of the percentage of cellulosic tissue in the inner zone (PercBluZ2) and the percentage of sclerenchyma in the outer zone (PercScIz1). Type III test was used. DF: degree of freedom, R²: coefficient of determination, CV : coefficient of variation, Root MSE: root mean squared error, Mean : trial mean (μ).

Biomass	PercBluZ2				PercScIz1			
	Source	DF	FValue	ProbF	Source	DF	FValue	ProbF
Miscanthus	Reagent	1	0.58	0.5857	Reagent	1	0.95	0.5077
	Temperature	1	3.02	0.3322	Temperature	1	1.62	0.4238
	Duration	12	8.41	<.0001	Duration	12	5.97	<.0001
	Reagent*Temp	1	88.59	<.0001 ⁽¹⁾	Reagent*Temp	1	643.11	<.0001 ⁽¹⁾
	R²	CV	Root MSE	Mean	R²	CV	Root MSE	Mean
	0.86	27.04	15.33	56.68	0.97	13.11	4.80	36.64
Sorghum	Reagent	1	0.77	0.5406	Reagent	1	218.7	<.0001
	Temperature	1	4.49	0.2807	Temperature	1	237.89	<.0001
	Duration	21	18.92	<.0001	Duration	21	12.11	<.0001
	Reagent*Temp	1	19.91	<.0001 ⁽¹⁾	Reagent*Temp	1	2.56	0.1117 ⁽²⁾
	R²	CV	Root MSE	Mean	R²	CV	Root MSE	Mean
	0.78	21.67	15.59	71.93	0.82	16.71	4.41	26.42

⁽¹⁾The significant Reagent*Temperature interaction is used to test Reagent and Temperature effects.

⁽²⁾The Reagent*Temperature interaction is not significant. The default residual is used to test Reagent and Temperature effects.

For the following, result analysis is focused on pretreatments carried out at 55°C for 24 h.

2. Links between histochemical parameters and biochemical composition and methane production

2.1. Impact of alkaline pretreatments on biochemical composition and methane production

Table 3 provides biochemical composition and methane production of raw and 55°C-pretreated internodes. Regarding the raw biomass, miscanthus is more lignified than sorghum. After pretreatments, the Klason lignin was removed up to 7% for sorghum and 29% for miscanthus. For both, NaOH was more efficient in removing lignin than CaO. The cellulose and hemicellulose contents were removed up to 31 and 24%, 11 and 40% for sorghum and

miscanthus, respectively. The LOI showed a larger increase after the CaO than with the NaOH pretreatment. The methane production improved by 5% for sorghum (CaO or NaOH pretreatments) and 15 and 8% for miscanthus pretreated with CaO and NaOH, respectively. The first order kinetics constant was improved up to 162% and 546% for sorghum and miscanthus, respectively.

Table 3: Comparative biochemical composition, LOI, methane production and first order kinetics constant of sorghum and miscanthus stem internode biomass: Influence of pretreatment.

	Cellulose (%TS)	Hemicelluloses (%TS)	Klason lignin (%TS)	LOI	Methane Production (NmL _{CH4} .g _{VS} ⁻¹)	k (d ⁻¹)
Raw sorghum	31.0 ± 0.5	15.2 ± 0.5	18.7 ± 0.5	1.13 ± 0.07	241 ± 17	0.097 ± 0.010
S CaO 55°C	27.1 ± 0.1	11.5 ± 0.4	14.4 ± 1.5	1.35 ± 0.01	254 ± 5	0.254 ± 0.013
S NaOH 55°C	21.4 ± 0.1	12.5 ± 0.3	10.4 ± 1.3	1.18 ± 0.1	253 ± 32	0.205 ± 0.005
Raw miscanthus	40.3 ± 0.1	15.8 ± 0.7	24.9 ± 1.4	0.90 ± 0.1	201 ± 18	0.046 ± 0.002
M CaO 55°C	36.0 ± 1.3	14.2 ± 0.1	19.4 ± 1.2	1.13 ± 0.03	231 ± 16	0.232 ± 0.041
M NaOH 55°C	36.2 ± 0.5	14.7 ± 0.6	14.9 ± 0.6	0.91 ± 0.02	218 ± 6	0.206*

*the duplicate had abnormal kinetics

2.2. Links between histochemical parameters and biochemical composition and methane production

Figure 4 presents the results of the PCA which investigated the dependence between the biochemical composition of raw and pretreated internodes and their methane production, first order kinetics constant and image analysis results. The first two principal components (PC) accounted for 88.7% of the total variability.

Fig. 4: Principal component analysis (PCA) plot of variables that are relative to the methane potential (MP), the first order kinetics constant (k), the biochemical composition (Cellulose, Hemi and LK: hemicellulose and Klason lignin) and the cellulose crystallinity (LOI). PercSclZ1 and PercBluZ2 were considered as additional variables.

The first PC accounted for 72.4% of the variation in the correlation matrix. The methane potential (MP) was anti-correlated to the cellulose and the Klason lignin content. The first order kinetics constant was anti-correlated to the hemicelluloses content. The analysis of the biochemical composition was made only on the solids matter. Consequently, MP and k were anti-correlated to the hemicelluloses and cellulose contents which remained in the matter after the pretreatment, they were thus correlated to their solubilisation. Moreover, MP and k particularly were anti-correlated with the Klason lignin content. The second PC accounted for 16.3% of the variability. The MP and the LOI were correlated. The decrease of the cellulose crystallinity improves its biodegradability. The parameter PercSclZ1 of the image analysis was correlated with the hemicelluloses and the Klason lignin contents. The decrease of the lignified sclerenchyma in Z1 made possible the solubilisation of the hemicelluloses by the degradation of the lignin.

Boon et al. (2008) showed that the distinctions regarding digestibility between internodes and the differences between maize cultivars are associated with differences in relative abundance of VB and sclerenchyma, in cell wall thickness, cell wall content and cell wall composition [40]. In the case of the corn stover, the sclerenchyma represents around 70% of the mass fractions [41]. Consequently, the variable PercSclZ1 is very informative.

This can possibly be explained by the fact that the sclerenchyma cells have a very thick wall and a low diameter whereas the Z2 parenchyma cells, which are originally red (in raw

biomass) and turn blue (unmasking of cellulose), have thin walls and a larger diameter offering a higher contact area. PercBluZ2 was correlated with the methane production kinetics. Cellulose became accessible as shown on the results of the staining procedures (because it was disembedded from the lignin which was removed by alkaline reagents) and its crystallinity decreased. Consequently, more cellulose was accessible and this degradation was faster.

FASGA is a very effective staining as it allows lignin and holocellulose visualization in a single step. However, because FASGA is not highly specific of lignin and cellulose, other complementary histochemical stainings were used to better understand the alkaline pretreatments mechanisms on tissues.

These stainings were applied to internodes pretreated at 55°C for 24 h (in order to compare two contrasted samples: raw and pretreated).

3 Histochemical characterization of lignins in the different internode tissues and influence of pretreatments on their location

Figure 5 illustrates lignin location (in red after phloroglucinol staining, in red or brown after Mäule staining) on raw and pretreated sorghum and miscanthus internode sections.

The obtained results confirmed the location of the lignin observed with FASGA on raw sorghum and miscanthus stem internodes.

With phloroglucinol staining, in Z1, the epidermis, the subepidermal and perivascular sclerenchyma were entirely red proving that they had cell walls with high lignin content. (Fig. 5a A, B, G, H). The sclerenchyma around the VB located in Z1 (Fig. 5a A, C, E) is thicker than the perivascular sclerenchyma of the vascular bundles located in the inner internode zone (Z2, Fig. 5a B, D, F). In this zone, the parenchyma was not lignified, it was entirely holocellulosic. Inside the vascular bundles, as expected, the xylem was highly stained in red by contrast with

phloem known to have cellulosic cell walls (Fig. 5a B, D, F). Moreover, miscanthus seems to be more lignified than sorghum (Fig. 5a A compared to Fig. 5a G).

Fig. 5: Comparison of lignin *in situ* localization between untreated sorghum or miscanthus stem internode sections after the alkaline pretreatments for 24 h at 55°C. Total lignin appears in red after tissue stained with phloroglucinol (a) G and S type lignins appear in brown and red, respectively after Mäule staining (b). A, C, E, G, I, K M, O, Q, S, U and W were in Z1, the others in Z2. Ep = epidermis, Sescl= subepidermal sclerenchyma, Pscl= perivascular sclerenchyma, Xyl= xylem, Phl=Phloem, Par= parenchyma

After pretreatments, there was a sharp decrease in the red color intensity in all lignified tissues except epidermis, for both miscanthus and sorghum (Fig. 5 C, F compared to Fig. 5a A, B and Fig. 5a I, L to Fig. 5a G, H). This reflects a possible attack of lignin by alkaline solutions which appears to be lower in miscanthus after treatment with CaO than with NaOH (Fig. 5a C, D, I, J and Fig. 5a E, F, K, L). This suggests that degradation of lignified cell walls is more effective after NaOH pretreatment than after CaO pretreatment.

A strong coloration after Mäule staining was present in Z1 at the level of the epidermis, the subepidermal and the perivascular sclerenchyma (Fig. 5b M, S). The G-type lignins are colored in orange-brown and the S-type lignins in red. These colors were also in Z2 located in VB (Fig. 5b N, T). However, the staining distribution was different for the two biomass. Indeed, the staining result was a more orange-brown color than red color regarding the epidermis, perivascular sclerenchyma in Z1 of miscanthus internodes and in Z2 VB. Miscanthus is richer in G-type lignins than sorghum and contains more G-type lignins than S-type lignins.

Villaverde et al. (2009) found that *M. x giganteus* presented a low S/G ratio (0.7) [42]. At tissue scale, the composition of the lignin was different according to the biomass type and its location.

After alkaline pretreatment, the coloration changed. The epidermis, xylem and perivascular parenchyma of the VB located in the inner stem zone (Z2) of miscanthus stem remained brown (Fig. 5b U to X). For sorghum only, the G-type lignin types remained brown in the inner VB of the Z2 (Fig. 5b P, R). However, in Z1, in the perivascular sclerenchyma of sorghum and miscanthus, the orange-brown staining disappeared, leading to predominant red colored areas (Fig. 5b O, Q, U, W). These results indicate that some G-type lignins were degraded by the alkaline solution. This selective degradation and the fact that more lignin was degraded in miscanthus could explain the improvement of miscanthus BMP. Moreover, Li et al. (2014) studied NaOH effects on three standard pairs of *Miscanthus* accessions that revealed three distinct monolignol (G, S, H) compositions but similar biochemical composition [24]. After NaOH pretreatment (0.5%, 1%, 4%, 8%, w/v, 50°C for 2 h), G-rich samples showed more effective extraction of lignin–hemicellulose complexes than the S- and H-rich samples. Moreover, after an enzymatic hydrolysis, G-rich biomass samples, rather than the H- or S-rich samples, can be completely hydrolyzed by cellulase enzymes into soluble sugars after the 4% NaOH pretreatment at 50 °C for 2 hours. The increased biomass enzymatic digestibility in the G-rich samples was attributed to efficient lignin extraction from the alkali pretreatments. Comparing internodes pretreated with CaO or NaOH, the phloroglucinol staining was lower with NaOH. Once again, the pretreatment using NaOH is suggested more efficient to degrade lignified tissues.

Phloroglucinol staining showed a high decrease of lignin in the xylem and in the perivascular sclerenchyma cells in Z2. Maïle reagent allowed to specify that lignin which remains after alkaline pretreatment corresponds mainly to S-type lignin in Z1 and to G-type lignin in Z2. In addition, these two staining methods highlight that, after alkaline pretreatments,

the epidermis seemed to be unaffected. The epidermis is a very specialized tissue rich in lignin but also in suberin and cuticle composed of cutin and waxes [43]. The cuticle is a hydrophobic surface layer. Cutin is typically composed of interesterified hydroxyl fatty acids, with lesser amounts of glycerol, phenyl- propanoids, and dicarboxylic acids [44]. Waxes are derived from very-long-chain fatty acids including alkanes, aldehydes, primary and secondary alcohols, ketones, and esters [45]. Due to these different lipidic components, the epidermis is a barrier against diffusion water loss and microbial invasion [46]. This is such a strong structure that even after anaerobic digestion, its high-silicified part remained unbroken [47].

4 Histochemical characterization of cellulose and crystalline cellulose location; influence of pretreatments on their availability for methane production

4.1 Total cellulose: Congo red staining

Figure 6 reveals the location of cellulose in internodes as a result of the Congo red staining. The Congo red staining on raw biomass revealed that highly lignified tissues such as the epidermis, the subepidermal sclerenchyma and the perivascular sclerenchyma are not stained in red (Fig. 5 A, G). In those tissues cellulose is probably masked by lignin. Only phloem and parenchyma cells of the Z2 (Fig. 5 B, H) and Z1 are known to have cellulosic or poorly lignified cell walls stained in Congo red.

Fig. 6: Raw and pretreated (with NaOH or CaO for 24h at 55°C) sorghum and miscanthus stem internode cross sections stained with Congo Red. Ep = epidermis, Sescl= subepidermal sclerenchyma, Pscl= périvascular sclerenchyma, Mxyl= metaxylem, Phl= Phloem

After alkaline pretreatments, there was a strong increase in Congo red staining affecting all tissues except the epidermis, the subepidermal sclerenchyma and part of the perivascular

sclerenchyma surrounding the vascular bundles located inside the Z1 (Fig. 6 C, E, I, K). The increase in the Congo red staining intensity, which marks the cellulose after alkaline pretreatment, must be related to the degradation of lignin, which would thus allow unmasking of cellulose. In VB in Z2, metaxylem became slightly red. It could suggest that metaxylem was a mixture of lignin and cellulose. The intensity of the staining was different between the two pretreatments. The staining result was more intense for NaOH than for CaO.

Taken as whole, histochemistry results are consistent with FASGA staining ones. They show that alkaline treatments attack lignin of certain tissues such as the xylem and the sclerenchyma around the vascular bundles located inside Z2, and in a lower extent inside Z1 (Fig. 2 and 6).

Li et al. (2018) divided sorghum stems in different fractions separating the pith from epidermis and outer rind and from VB and inner rind [48]. The fractions isolated from the pith parenchyma were the least recalcitrant to mild alkaline pretreatments; epidermis and the outer rind were the most. Because the miscanthus was more lignified, the unmasking of the cellulose was more substantial.

4.2 Mapping crystalline cellulose using immunolocation with CBM

In Figure 7, cellulose crystallinity is shown by the yellow fluorescence signal. On raw stem internodes, in accordance with what was expected, the signal is strongly located in the cell walls of the parenchyma of Z2 and in those of the Z1. It is absent from the vascular bundles except within the phloem. When present, the signal which represents cellulose in its crystalline form is arranged homogeneously and regularly along the walls (Fig. 7 A, B, G, H).

Fig. 7: Influence of alkaline pretreatments on crystalline cellulose *in situ* localisation: Raw and pretreated sorghum and miscanthus stem internode cross sections after the alkaline

pretreatments during 24h at 55°C with CBM. The first column corresponds to raw sorghum, the second one to pretreated sorghum with CaO at 55°C for 24 h and the third to sorghum pretreated with NaOH at 55°C for 24 h.

After alkaline pretreatments of sorghum and miscanthus tissues, a significant drop in fluorescence intensity occurred, and this signal, when present, is no longer homogeneously distributed, but is in the form of irregular clusters concentrated in certain areas of the cellulosic cell walls (Fig. 7 C-F, I-L). In Z2, the cell walls of parenchyma cells were thin and the fluorescence was homogeneous (Fig. 7).

Alkaline pretreatment reduced the crystallinity of cellulose (Fig. 7) and thus slackened the cellulose fibers (Figs. 2 and 6). The evolution of the fluorescence location implied the evolution of the biomass tissue structure. Cellulose became more amorphous and thus more biodegradable. This result has to be confronted with the biochemical composition of pretreated samples. In particular, LOI increase after pretreatment (Table 3) may be interpreted by the degradation of amorphous cellulose, leading to an increase in the crystalline zone percentage. However, histological results also reveal the reduction in crystalline cellulose, to a larger extent after soda pretreatment. Thus it can be concluded that soda pretreatment led to the degradation of both amorphous and crystalline cellulose. This is consistent with the literature, indeed, alkaline pretreatments were highlighted to decrease the crystallinity of cellulose [49].

Conclusions

This study demonstrates the interest of histochemical approaches to decipher the effect of pretreatments on the cellular and macromolecular architecture of biomass and on its digestibility by anaerobic digestion microbial consortia. This *in situ* approach complements the information obtained from *in vitro* biochemical analysis. These results demonstrate that NaOH and CaO pretreatments affected all the internode tissues (parenchyma, sclerenchyma, xylem),

except the epidermis and the inner sclerenchyma around the vascular bundles. At a macromolecular level, the data obtained from this study showed that alkaline treatments have a versatile effect. Indeed, they cause i) the delignification of lignified walls, which leads to cellulose unmasking, ii) hemicellulose and cellulose degradation, and iii) a decrease in crystalline cellulose along cell walls. These macromolecular parietal rearrangements are accompanied by an increase in the parenchyma cell wall thickness. In all likelihood, this reflects the relaxation of the pectocellulosic walls and the decrease in their cohesion with a tendency to separate parenchyma cells. The degradation of the lignin was different according to its units (S-type lignin less degraded than G-type lignin) and their tissular location. The higher pretreatment effectiveness on *Miscanthus x giganteus* Floridulus methane potential than on Sorghum Biomass 140 may be explained by the higher lignin content in *Miscanthus x giganteus* and the strong degradation of lignins (especially G-type lignins) during alkali pretreatments.

Acknowledgements

Particular acknowledgements are addressed to Dr Arnoult Stéphanie (INRA UE0972 GCIE) and Dr Pot David (CIRAD-AGAP) who provided the raw miscanthus and sorghum stems, respectively. We thank Bio2E platform (doi:10.5454/1.557234103446854E12) and the MRI imaging facility, which is part of the UMS BioCampus Montpellier and a member of the national infrastructure, France-BioImaging, (www.mri.cnrs.fr, www.france-bioimaging.org) for providing facilities to perform experiments.

Declarations

Funding: This work was supported by the project Biomass For the Future from the French National Research Agency (ANR, grant ANR-11-BTBR-0006-BFF).

Conflicts of interest/Competing interests: The authors declare that they have no known competing financial interests or personal

relationships that could have appeared to influence the work reported in this paper.

Availability of data and material: Authors will make data available on request

Code availability: Not applicable

Authors' contributions

Hélène Laurence Thomas: Investigation, Formal analysis, Visualization, Conceptualization, Writing – Original Draft

Helga Felix P. Nolasco: Investigation, Writing - Review & Editing.

Hélène Carrère: Funding acquisition, Conceptualization, Supervision, Validation, Writing - Review & Editing.

Marc Lartaud: Formal analysis, Writing - Review & Editing

Tuong-Vi Cao: Formal analysis, Writing - Review & Editing.

Christelle Baptiste: Investigation.

Jean-Luc Verdeil: Conceptualization, Supervision, Validation, Writing - Review & Editing.

References

1. Ghatak HR (2011) Biorefineries from the perspective of sustainability: Feedstocks, products, and processes. *Renew Sustain Energy Rev* 15:4042–4052. <https://doi.org/10.1016/j.rser.2011.07.034>
2. Arnoult S, Obeuf A, Béthencourt L, et al (2015) Miscanthus clones for cellulosic bioethanol production: Relationships between biomass production, biomass production components, and biomass chemical composition. *Ind Crops Prod* 63:316–328. <https://doi.org/10.1016/j.indcrop.2014.10.011>
3. Monk RL, Miller FR, McBee GG (1984) Sorghum improvement for energy production. *Biomass* 6:145–153. [https://doi.org/10.1016/0144-4565\(84\)90017-9](https://doi.org/10.1016/0144-4565(84)90017-9)
4. Scheller H V, Pauly M, Loque D (2015) Engineering of plant cell walls for enhanced biofuel production. *Plant Biol* 25:151–161. <https://doi.org/10.1016/j.pbi.2015.05.018>
5. Mcfarlane HE, Anett D (2014) The Cell Biology of Cellulose Synthesis. 1–26. <https://doi.org/10.1146/annurev-arplant-050213-040240>
6. Pauly M, Gille S, Liu L, et al (2013) Hemicellulose biosynthesis. *Planta* 627–642. <https://doi.org/10.1007/s00425-013-1921-1>
7. Pu Y, Zhang D, Singh PM, Ragauskas AJ (2008) The new forestry biofuels sector. 2:58–73. <https://doi.org/10.1002/bbb>
8. Zheng Y, Zhao J, Xu F, Li Y (2014) Pretreatment of lignocellulosic biomass for enhanced biogas production. *Prog. Energy Combust. Sci.*42:35–53. <https://dx.doi.org/10.1016/j.pecs.2014.01.001>

9. Vanholme R, Demedts B, Morreel K, et al (2010) Lignin Biosynthesis and Structure 1. *Plant Physiol* 153:895–905. <https://doi.org/10.1104/pp.110.155119>
10. Baucher M, Monties B, Montagu M Van, Boerjan W (1998) Biosynthesis and Genetic Engineering of Lignin Biosynthesis and Genetic Engineering of Lignin. *CRC Crit Rev Plant Sci* 17:125–197
11. Wertz J-L, Bédué O (2013) Lignocellulosic Biorefineries
12. Monlau F, Barakat A, Trably E, et al (2013) Lignocellulosic Materials Into Biohydrogen and Biomethane: Impact of Structural Features and Pretreatment. *Crit Rev Environ Sci Technol* 43:260–322. <https://doi.org/10.1080/10643389.2011.604258>
13. Kikas T, Tutt M, Raud M, et al (2016) Basis of energy crop selection for biofuel production: Cellulose vs . lignin. *Int J Green Energy* 49–54. <https://doi.org/10.1080/15435075.2014.909359>
14. Karimi K, Shafiei M, Kumar R (2013) Progress in Physical and Chemical Pretreatment of Lignocellulosic Biomass
15. Bichot A, Delgenès J-P, Méchin V, et al (2018) Understanding biomass recalcitrance in grasses for their efficient utilization as biorefinery feedstock. *Rev Environ Sci Bio/Technology* 17:707–748. <https://doi.org/10.1007/s11157-018-9485-y>
16. Ravindran R, Jaiswal AK (2016) A comprehensive review on pre-treatment strategy for lignocellulosic food industry waste: Challenges and opportunities. *Bioresour. Technol.* <https://doi.org/10.1016/j.biortech.2015.07.106>
17. Rollin JA, Zhu Z, Sathitsuksanoh N, Zhang YP (2011) Increasing Cellulose Accessibility Is More Important Than Removing Lignin : A Comparison of Cellulose Solvent-Based Lignocellulose Fractionation and Soaking in Aqueous Ammonia. *Biotechnol Bioeng* 108:22–30. <https://doi.org/10.1002/bit.22919>
18. Monlau F, Sambusiti C, Barakat A, et al (2012) Predictive models of biohydrogen and biomethane production based on the compositional and structural features of lignocellulosic materials. *Environ Sci Technol* 46:12217–12225. <https://doi.org/10.1021/es303132t>
19. Carrere H, Antonopoulou G, Affes R, et al (2016) Review of feedstock pretreatment strategies for improved anaerobic digestion: From lab-scale research to full-scale application. *Bioresour Technol* 199:386–397. <https://doi.org/http://dx.doi.org/10.1016/j.biortech.2015.09.007>
20. Monlau F, Barakat A, Steyer JP, Carrere H (2012) Comparison of seven types of thermo-chemical pretreatments on the structural features and anaerobic digestion of sunflower stalks. *Bioresour Technol* 120:241–247. <https://doi.org/10.1016/j.biortech.2012.06.040>
21. Talebnia F, Karakashev D, Angelidaki I (2010) Production of bioethanol from wheat straw: An overview on pretreatment, hydrolysis and fermentation. *Bioresour Technol* 101:4744–4753. <https://doi.org/10.1016/j.biortech.2009.11.080>
22. Hernández-Beltrán JU, Hernández-De Lira IO, Cruz-Santos MM, et al (2019) Insight into pretreatment methods of lignocellulosic biomass to increase biogas yield: Current state, challenges, and opportunities. *Appl Sci* 9:3721.

<https://doi.org/10.3390/app9183721>

23. Thomas HL, Arnoult S, Brancourt-hulmel M, Carrère H (2019) Methane Production Variability According to Miscanthus Genotype and Alkaline Pretreatments at High Solid Content. *BioEnergy Res* 12:325–337. <https://doi.org/10.1007/s12155-018-9957-5>
24. Li M, Si S, Hao B, et al (2014) Mild alkali-pretreatment effectively extracts guaiacyl-rich lignin for high lignocellulose digestibility coupled with largely diminishing yeast fermentation inhibitors in Miscanthus. *Bioresour Technol* 169:447–454. <https://doi.org/10.1016/j.biortech.2014.07.017>
25. Sambusiti C, Ficara E, Malpei F, et al (2013) Effect of sodium hydroxide pretreatment on physical, chemical characteristics and methane production of five varieties of sorghum. *Energy* 55:449–456. <https://doi.org/10.1016/j.energy.2013.04.025>
26. Nkongndem Nkemka V, Yongqiang L, Hao X (2016) Effect of thermal and alkaline pretreatment of giant miscanthus and Chinese fountaingrass on biogas production. *Water Sci Technol* 849–856. <https://doi.org/10.2166/wst.2015.559>
27. Karimi K, Taherzadeh MJ (2016) A critical review of analytical methods in pretreatment of lignocelluloses: Composition, imaging, and crystallinity. *Bioresour Technol* 200:1008–1018. <https://doi.org/10.1016/j.biortech.2015.11.022>
28. Thomas HL, Pot D, Latrille E, et al (2019) Sorghum Biomethane Potential Varies with the Genotype and the Cultivation Site. *Waste and Biomass Valorization* 10:783–788. <https://doi.org/10.1007/s12649-017-0099-3>
29. Sambusiti C, Ficara E, Malpei F, et al (2012) Influence of alkaline pre-treatment conditions on structural features and methane production from ensiled sorghum forage. *Chem Eng J* 211–212:488–492. <https://doi.org/10.1016/j.cej.2012.09.103>
30. Pomar F, Merino F, Barceló AR (2002) O-4-linked coniferyl and sinapyl aldehydes in lignifying cell walls are the main targets of the Wiesner (phloroglucinol-HCl) reaction. *Protoplasma* 220:17–28. <https://doi.org/10.1007/s00709-002-0030-y>
31. Iiyama K, Pant R (1988) The mechanism of the Mäule colour reaction introduction of methylated syringyl nuclei into softwood lignin. *Wood Sci Technol* 22:167–175. <https://doi.org/10.1007/BF00355852>
32. Blake AW, McCartney L, Flint JE, et al (2006) Understanding the biological rationale for the diversity of cellulose-directed carbohydrate-binding modules in prokaryotic enzymes. *J Biol Chem* 281:29321–29329. <https://doi.org/10.1074/jbc.M605903200>
33. Hernandez-Gomez MC, Rydahl MG, Rogowski A, et al (2015) Recognition of xyloglucan by the crystalline cellulose-binding site of a family 3a carbohydrate-binding module. *FEBS Lett* 589:2297–2303. <https://doi.org/10.1016/j.febslet.2015.07.009>
34. Perrier L, Rouan L, Jaffuel S, et al (2017) Plasticity of Sorghum Stem Biomass Accumulation in Response to Water Deficit: A Multiscale Analysis from Internode Tissue to Plant Level. 8:1–14. <https://doi.org/10.3389/fpls.2017.01516>
35. APHA American Public Health Association (1998) Standard Methods for the Examination of Water and Wastewater

36. A. Sluiter, B. Hames, R. Ruiz, et al (2011) Determination of Structural Carbohydrates and Lignin in Biomass Laboratory Analytical Procedure (LAP)
37. Tukey J (1949) Comparing Individual Means in the Analysis of Variance. *Biometrics* 5 (2):99–114
38. Kaack K, Schwarz KU, Brander PE (2003) Variation in morphology, anatomy and chemistry of stems of *Miscanthus* genotypes differing in mechanical properties. *Ind Crops Prod* 17:131–142. [https://doi.org/10.1016/S0926-6690\(02\)00093-6](https://doi.org/10.1016/S0926-6690(02)00093-6)
39. Ji Z, Zhang X, Ling Z, et al (2016) Tissue specific response of *Miscanthus* × *giganteus* to dilute acid pretreatment for enhancing cellulose digestibility. *Carbohydr Polym* 154:247–256. <https://doi.org/10.1016/j.carbpol.2016.06.086>
40. Boon EJM., Struick P., Tamminga S, et al (2008) Stem characteristics of two forage maize (*Zea mays* L .) cultivars varying in whole plant digestibility . III . Intra-stem variability in anatomy, chemical composition and in vitro rumen fermentation. *NJAS - Wageningen J Life Sci* 56:101–122. [https://doi.org/10.1016/S1573-5214\(08\)80019-X](https://doi.org/10.1016/S1573-5214(08)80019-X)
41. Sun L, Li C, Xue Z, et al (2013) Unveiling high-resolution, tissue specific dynamic changes in corn stover during ionic liquid pretreatment. *RSC Adv* 3:2017–2027. <https://doi.org/10.1039/c2ra20706k>
42. Villaverde JJ, Li J, Ek M, et al (2009) Native Lignin Structure of *Miscanthus* x *giganteus* and Its Changes during Acetic and Formic Acid Fractionation. *J Agric Food Chem* 57:6262–6270. <https://doi.org/10.1021/jf900483t>
43. Reina-Pinto JJ, Yephremov A (2009) Surface lipids and plant defenses. *Plant Physiol Biochem* 47:540–549. <https://doi.org/10.1016/j.plaphy.2009.01.004>
44. Kolattuduky P (2001) Polyesters in higher Plants. *Advances in Biochemical Engineering/Biotechnology*
45. Yeats TH, Rose JKC (2013) Topical Review on Cuticle Synthesis and Function The Formation and Function of Plant Cuticles 1. *Plant Physiol* 163:5–20. <https://doi.org/10.1104/pp.113.222737>
46. Norman GL, Michael GP (1989) *Plant Cell Wall Polymers, Biogenesis and Biodegradation*
47. Motte JC, Watteau F, Escudié R, et al (2015) Dynamic observation of the biodegradation of lignocellulosic tissue under solid-state anaerobic conditions. *Bioresour Technol* 191:322–326. <https://doi.org/10.1016/j.biortech.2015.04.130>
48. Li M, Yan G, Bhalla A, et al (2018) Physical fractionation of sweet sorghum and forage / energy sorghum for optimal processing in a biorefinery *Industrial Crops & Products* Physical fractionation of sweet sorghum and forage / energy sorghum for optimal processing in a biore fi nery. *Ind Crop Prod* 124:607–616. <https://doi.org/10.1016/j.indcrop.2018.07.002>
49. Li M, Wang J, Yang Y, Xie G (2016) Alkali-based pretreatments distinctively extract lignin and pectin for enhancing biomass saccharification by altering cellulose features in sugar-rich Jerusalem artichoke stem. *Bioresour Technol* 208:31–41. <https://doi.org/10.1016/j.biortech.2016.02.053>

Fig. 1: Example of image processing under ImageJ of sorghum transversal internode section. Z1 stands for Zone 1, it is the outer internode zone characterized with a high density of vascular bundles. Z2 is the internal zone, PercSlcZ1: percentage of lignified sclerenchyma area in Z1, PercBluZ2: percentage of cellulosic area available in Z2, densVBZ2: represents the density of vascular bundles in Z2.

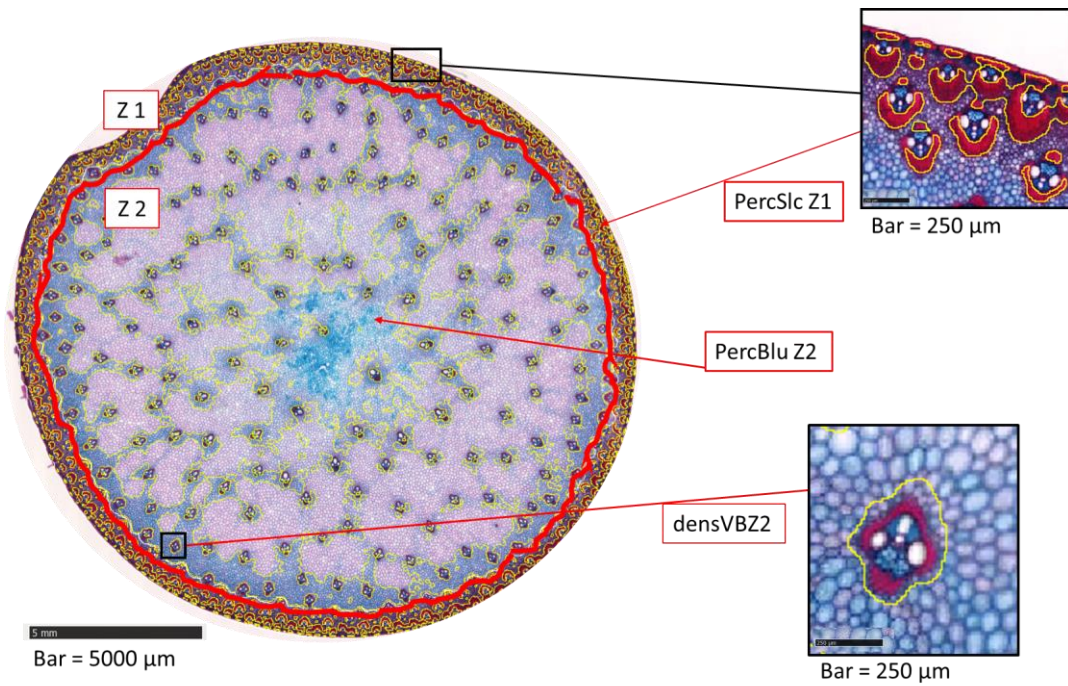


Fig. 2: Comparative effect of alkaline pretreatments on internode structure. For all the pretreatments, the duration was 24 hours. Observations were made after FASGA staining.

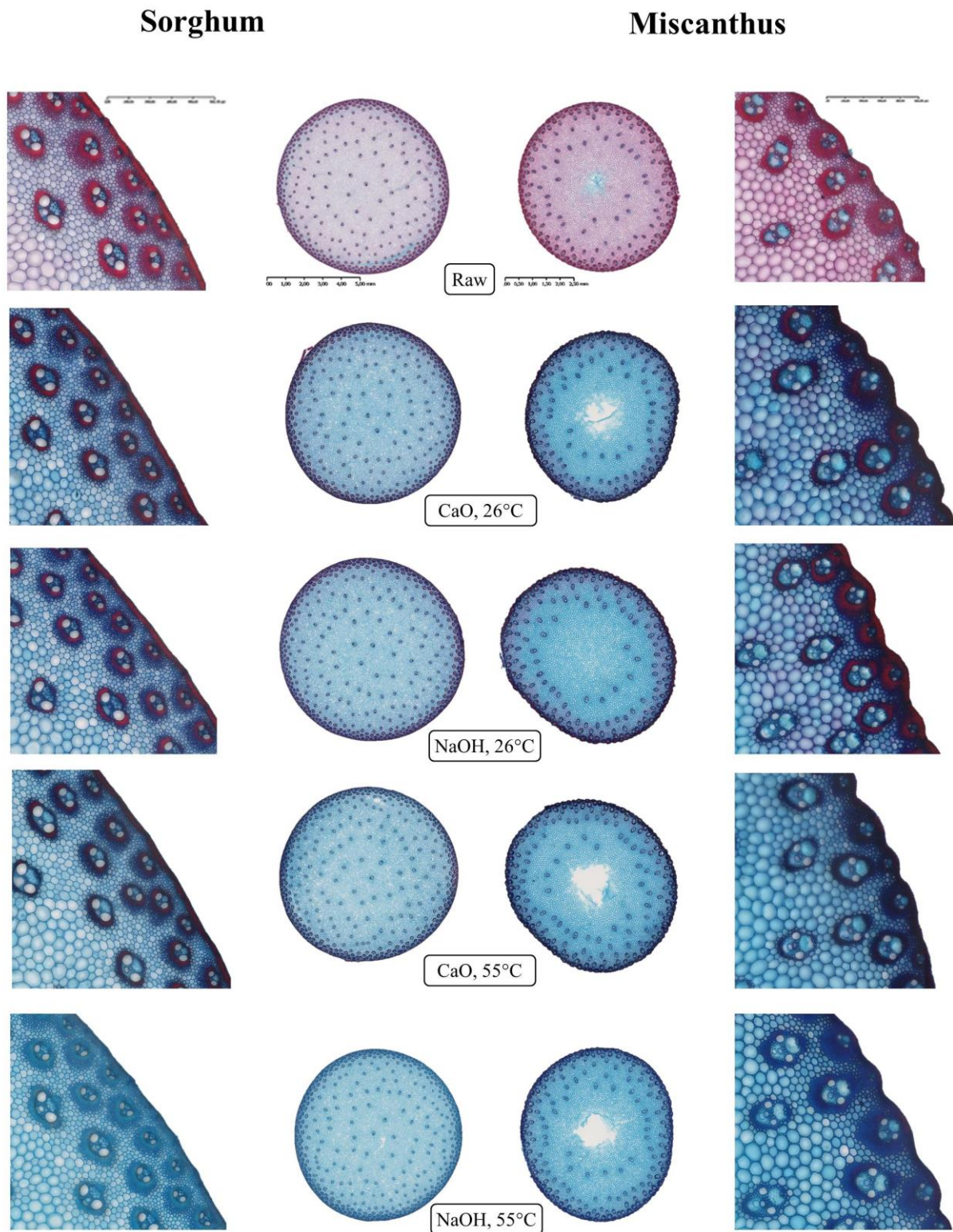
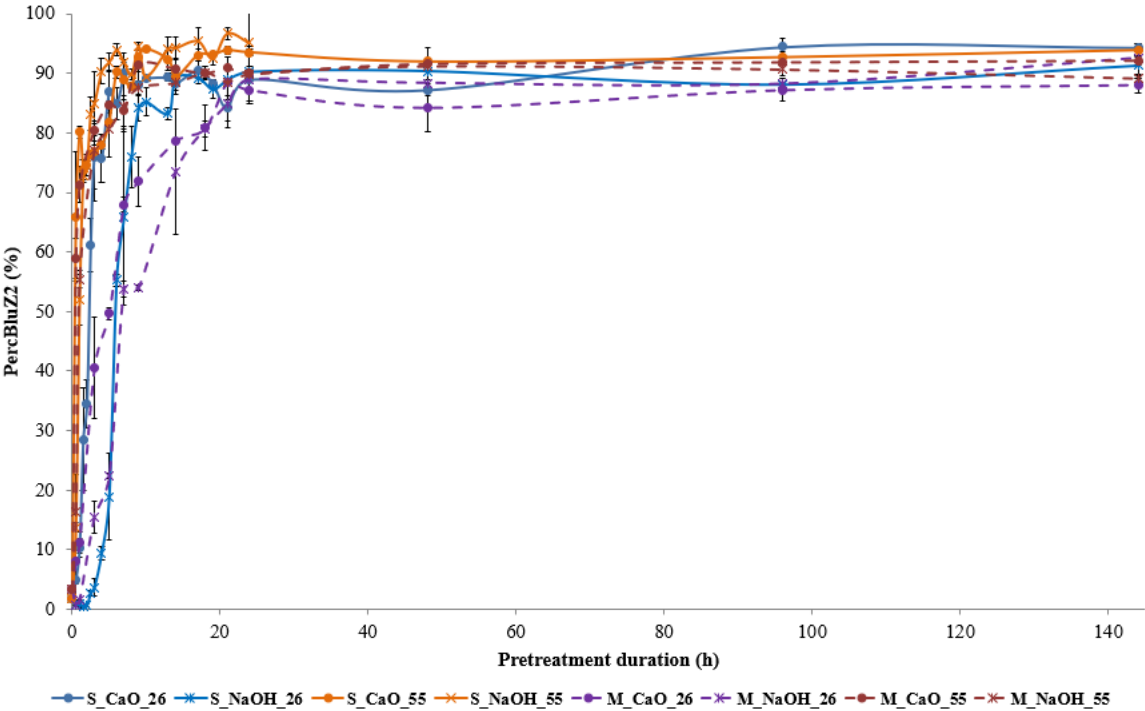
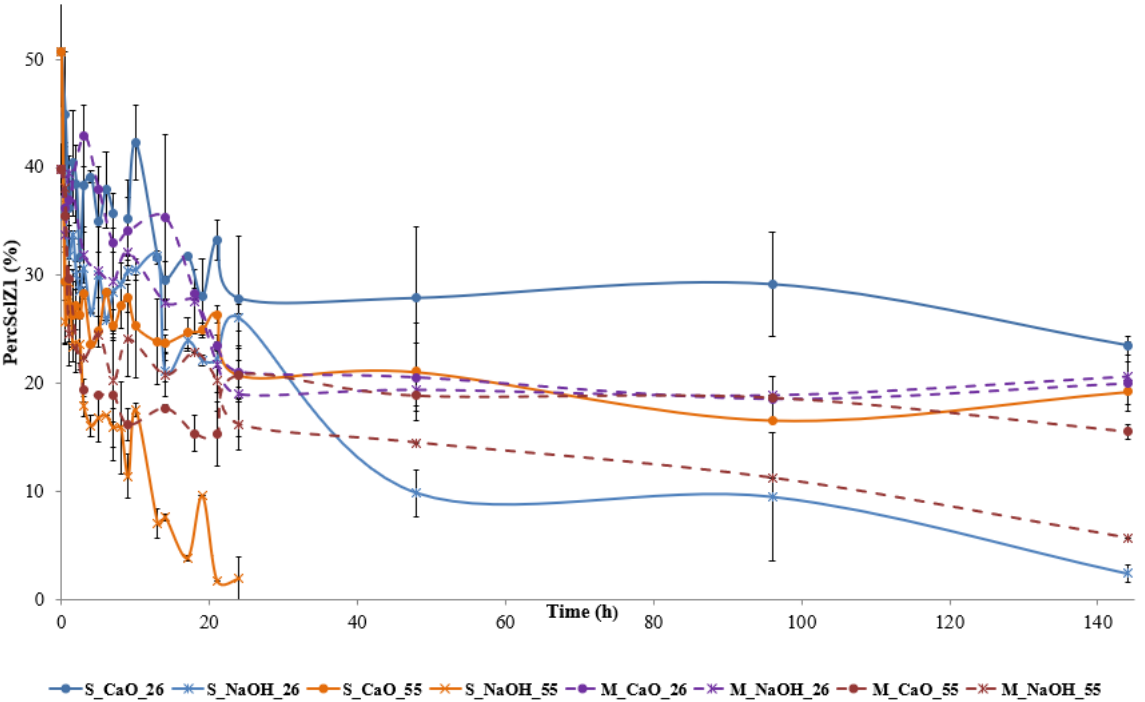


Fig. 3: Sorghum (S) and Miscanthus (M) biomass behavior during alkaline pretreatments: Influence of NaOH, CaO and temperature on the evolution of the cellulosic cells of the Z2 zone (PercBluZ2) (a) and on the lignified sclerenchyma in the outer internode zone (PercSclZ1) (b) from 0 to 144 h. Alkaline pretreatments were carried out at 26°C and 55 °C.



(a)



(b)

Fig. 4: Principal component analysis (PCA) plot of variables that are relative to the methane potential (MP), the first order kinetics constant (k), the biochemical composition (Cellulose, Hemi and LK: hemicellulose and Klason lignin) and the cellulose crystallinity (LOI). PercScIz1 and PercBluZ2 were considered as additional variables.

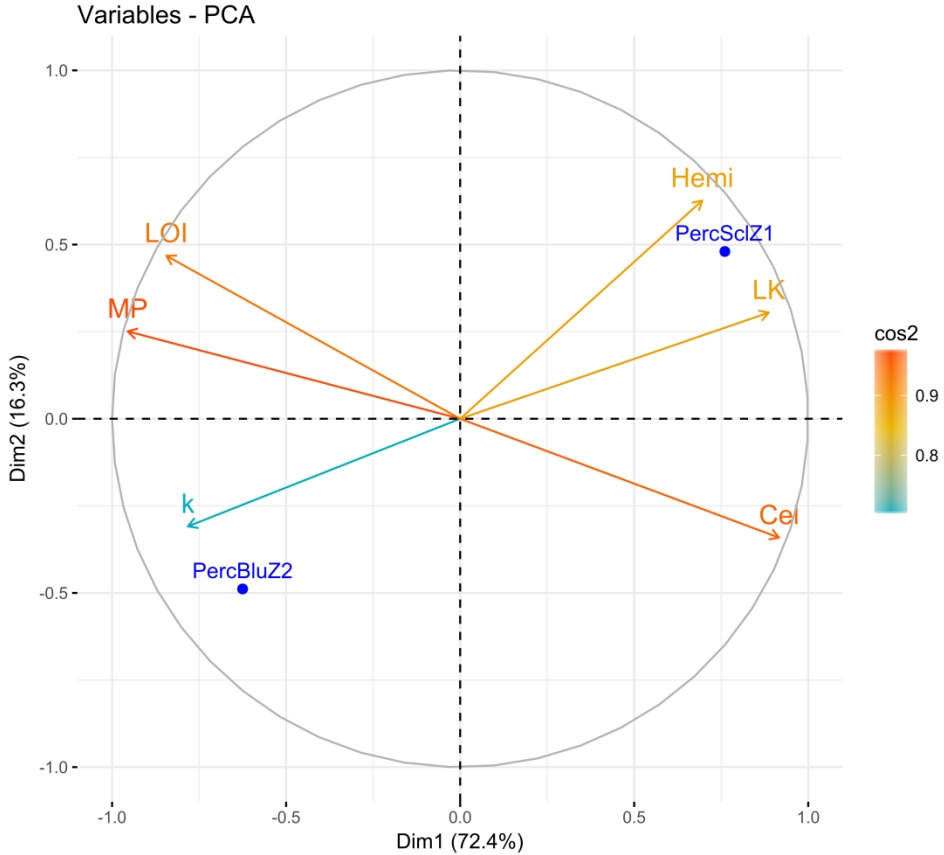


Fig. 5: Comparison of lignin *in situ* localization between untreated sorghum or miscanthus stem internode sections after the alkaline pretreatments for 24 h at 55°C. Total lignin appears in red after tissue stained with phloroglucinol (a) G and S type lignins appear in brown and red, respectively after Mäule staining (b). A, C, E, G, I, K M, O, Q, S, U and W were in Z1, the others in Z2. Ep = epidermis, Sesc1= subepidermal sclerenchyma, Pscl= perivascular sclerenchyma, Xyl= xylem, Phl=Phloem, Par= parenchyma.

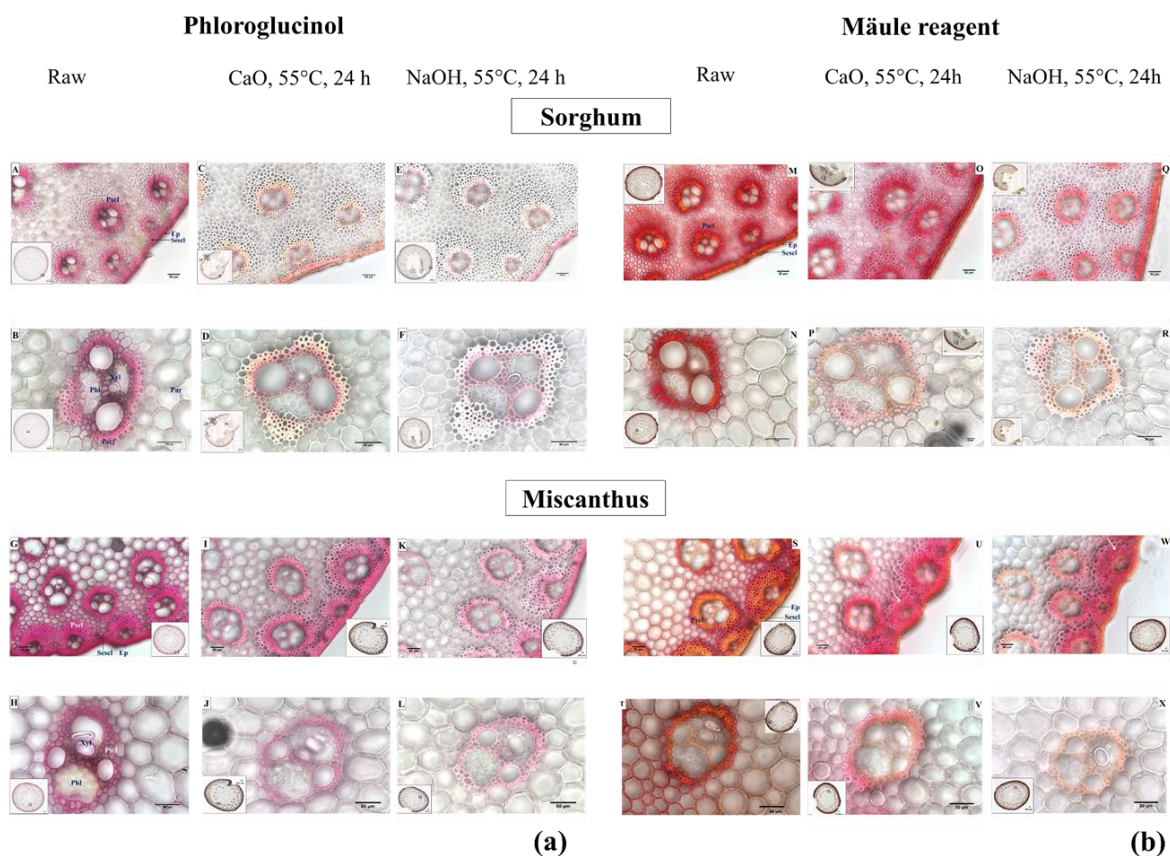


Fig. 6: Raw and pretreated (with NaOH or CaO for 24h at 55°C) sorghum and miscanthus stem internode cross sections stained with Congo Red. Ep = epidermis, Sesc= subepidermal sclerenchyma, Pscl= périvascular sclerenchyma, Mxyl= metaxylem, Phl= Phloem.

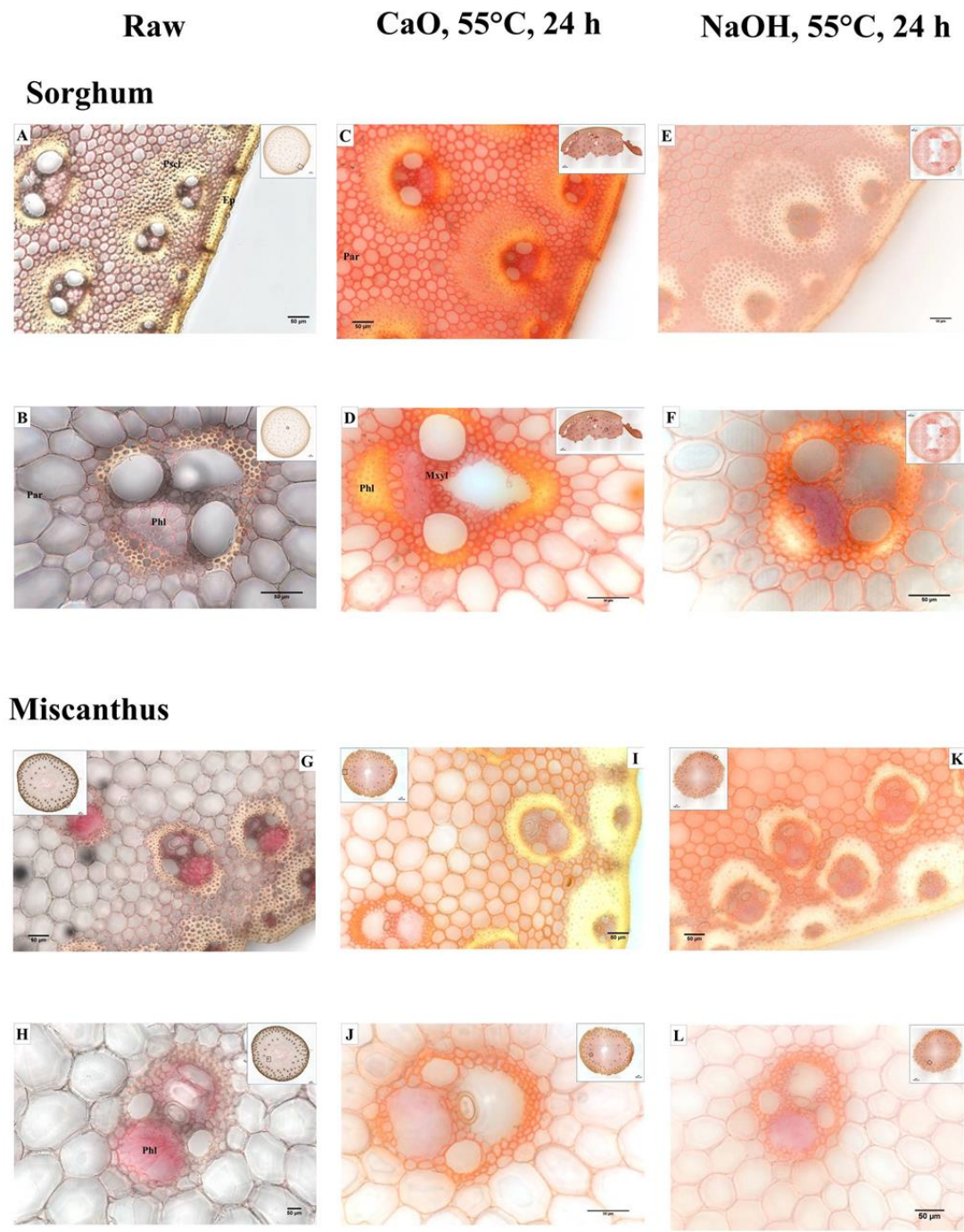


Fig. 7: Influence of alkaline pretreatments on crystalline cellulose *in situ* localisation: Raw and pretreated sorghum and miscanthus stem internode cross sections after the alkaline pretreatments during 24h at 55°C with CBM. The first column corresponds to raw sorghum, the second one to pretreated sorghum with CaO at 55°C for 24 h and the third to sorghum pretreated with NaOH at 55°C for 24 h.

